Оптический журнал

Биомедицинская оптика

Characterization of interaction between ligustroflavone and bovine serum albumin

© 2020 S. Sun, Z. Yuan, Y. Q. Lu

Analysis and Testing Centre, Dezhou University, Dezhou City Shandong Province, the P.R. China

E-mail: yuanqilu@126.com (Yuanqi Lu)

Submitted 12.12.2019

DOI:10.17586/1023-5086-2020-87-06-34-42

The interaction of ligustroflavone with bovine serum albumin was investigated by affinity capillary electrophoresis, ultraviolet visible absorption spectroscopy and fluorescence quenching methods in this ariticle. The affinity capillary electrophoresis gives binding constants (*Ka*) at near-physiological conditions. Mobility ratio (*M*) was selected to deduce the *Ka*, which effectively eliminates the influence of electroosmotic flow. The fluorescence quenching method provided quenching constant *Ksv*, binding site number *n* and binding constants *Kb*. The fluorescence results indicate that bovine serum albumin fluorescence quenching is mainly a static quenching process. The *Ka* value (7.1089×10^4) obtained from affinity capillary electrophoresis is in agreement with *Kb* (value is 8.0057×10^4) from fluorescence spectroscopy showing ligustroflavone has great affinity toward bovine serum albumin. Complex formed between ligustroflavone and bovine serum albumin was evident from the data of ultraviolet visible absorption spectroscopy which is consistent with the fluorescence static quenching result. And thermodynamic parameters of the negative ΔH and ΔS values obtained by affinity capillary electrophoresis showed that the van der Waals interactions and hydrogen bond played important roles in the binding of ligustroflavone to bovine serum albumin. The data obtained in this paper can help us in gaining some insights on a possible drug/protein interaction.

Keywords: *ligustroflavone, bovine serum albumin, affinity capillary electrophoresis, fluorescence spectroscopy, binding constants, thermodynamic parameters.*

OCIS codes: *300.0300, 300.6280, 300.6540, 300.6550, 000.1430, 000.6850.*

Характеризация взаимодействия лигустрофлавона с бычьим сывороточным альбумином

© 2020 г. Shan Sun, Zhe Yuan, Yuanqi Lu

Исследовалось взаимодействие лигустрофлавона с бычьим сывороточным альбумином методами аффинного капиллярного электрофореза по спектрам поглощения видимого и ультрафиолетового излучения и по тушению флуоресценции. Первый метод обеспечивает получение значений констант связывания *Ka* в условиях, близких к физиологическим. Выбранные значения отношения мобильностей M эффективно исключали влияние электроосмотического потока. Методом тушения флуоресценции определялись константа тушения *Ksv*, число связей *n* и константы связи *Kb*. Параметры флуоресценции свидетельствуют, что её тушение для бычьего сывороточного альбумина есть по преимуществу статический процесс. Значение *Ka*, измеренное методом аффинного капиллярного электрофореза (7.1089×10^4), оказалось близким к значению *Kb*,

полученному из флуоресцентых экспериментов (8.0057×10^4), что доказывает значительное сродство лигустрофлавона к сывороточному альбумину. Наличие комплекса, формируемого лигустрофлавином и бычьим сывороточным альбумином, является очевидным из согласия данных, полученных из спектров поглощения, с результатами по тушению флуоресценции. Отрицательный знак термодинамических параметров ΔH and ΔS показал, что ван-дер-ваальсовские взаимодействия и наличие водородных связей играют важную роль в связывании лигустрофлавона и бычьего сывороточного альбумина. Полученные данные могут помочь в выявлении возможных взаимодействий лекарственных препаратов с протеинами.

Ключевые слова: *лигустрофлавон, бычий сывороточный альбумин, аффинный капиллярный электрофорез, флуоресцентная спектроскопия, константы связывания, термодинамические параметры.*

1. INTRODUCTION

Serum albumin, carrying several endogenous and exogenous species, is an important transport protein of the body circulatory system [1, 2]. The investigation of binding between molecules and albumin has become an interesting research field in life sciences, chemistry and clinical medicine for searching interaction mechanism of biochemistry and drugs. Accounting for 60% of the plasma protein [3], human serum albumin (HSA) is the most abundant protein in human plasma system. HSA has many physiological functions such as its key role as a carrier of various endogenous and exogenous ligands to specific biological targets [4]. Thus HSA is nowadays recognized as a model protein for studying the drug/protein interaction. Bovine serum albumin (BSA) which is composed of a single polypeptide chain with 583 amino acid residues making up three homologous domains is an α-helicoidal globular protein [5, 6]. BAS has high homology and similarity to HSA in structure and conformation [7–9] and it has been one of the most extensively studied proteins to explore the interaction between drugs and serum albumin. Nowadays, natural products are attracting increasing attention for their reliable therapeutic effects in clinic [10]. Ligustroflavone (molecular structure is shown in Fig. 1) is an active flavonoid ingredient in Chinese herbal medicine of Shan Xiang Yuan Ye (Folium Turpinia). Its main pharmacology functions include anti-inflammatory, anti-bacterial and immune-regulating effects [11–13]. In recent years, more and more researches on ligustroflavone have been conducted. In 2010 edition of the Chinese Pharmacopoeia, ligustroflavone has been included as reference for the content determination of Shan Xiang Yuan Ye [14]. In order to provide a theoretical reference for the rational clinical application of ligustroflavone, the binding between it and BSA was studied in our work. Various methods have been reported in the literature for the study of drug-protein interaction, such as capillary electrophoresis (CE) [15], ultraviolet-visible (UV-Vis) absorption [16], infrared spectroscopy [17], fluorescence [18, 19] and electrochemistry [20]. Affinity capillary electrophoresis (ACE) as a fast, precise and parsimonious method [21–23] has been shown to be an efficient meth-

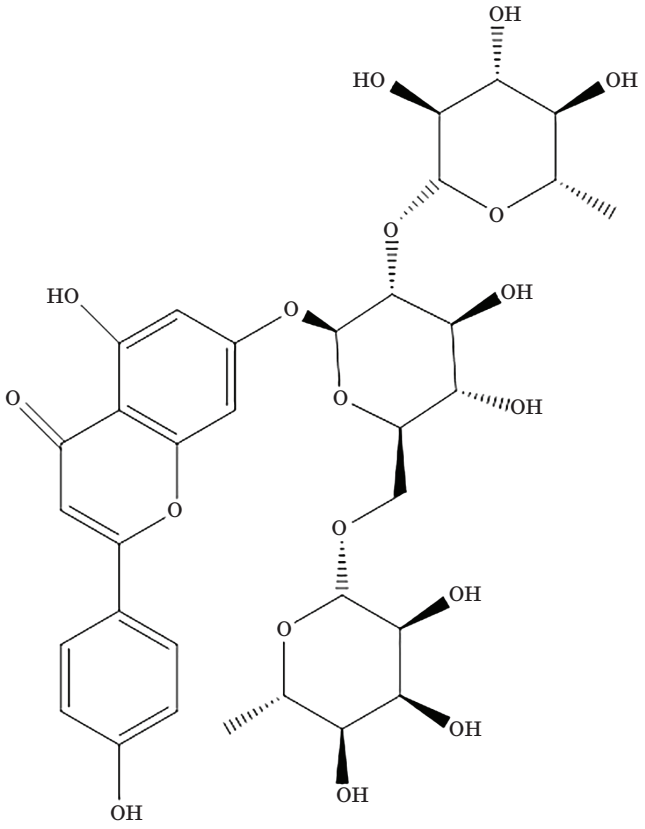

Fig. 1. The molecular structure of ligustroflavone.

od for the investigation of the interactions between small molecules and biomacromolecules [24]. It offers some advantages including low consumption of protein and drug, short analysis times and low purity requirement of analytes [25, 26]. Besides, binding constants of several samples can be estimated simultaneously and the separations can be carried out in solution near physiological buffer conditions, so the analyte can be preserved in a native state, and its molecular function can be maintained. Fluorescence spectroscopy and UV-Vis absorption spectroscopy has also been widely used to probe the affinity of biomolecules for its high sensitivity, high selectivity and ease of performance [27].

In this work, a simple ACE method was applied to study the interaction between ligustroflavone and BSA under physiological conditions. To further prove that the results were reliable, the fluorescence spectroscopy was also used in tandem with UV-Vis absorption spectroscopy. The experimental results showed that the binding constants and the number of binding sites obtained by electrophoresis are in well agreement with fluorescence spectroscopy. And it is reasonable that the data has a little difference obtained by different analytical techniques. The study in our work can provide useful information for better understanding the relationships between ligustroflavone and BSA.

2. EXPERIMENT

2.1. Instrument

All ACE experiments were carried out with a Beckman P/ACE MDQ system equipped with a photodiode array detector. Data were collected and analyzed with the Beckman 32 Karat Software (version 7.0). A 64.5 cm (54 cm to the detector) × 75 μm (i.d.) uncoated fused-silica capillary (Yongnian reafine chromatography equipment, P. R. China) was utilized. The fluorescence analysis was carried out using a F-4600 spectrofluorometer (Hitachi, Japan). The UV-vis absorption spectra were attained with a UV-2450 spectrophotometer (Shimadzu, Japan). PHSJ-4A meter (Shanghai Precision & Scientific Instrument Co., Shanghai, China) were used in sample treatment.

2.2. Chemicals and solutions

Ligustroflavone was purchased from Shanghai Yuan Ye Biological Technology company (Shanghai, China). BSA were obtained from Shanghai Han Si Chemical Company (Shanghai, China). Disodium hydrogen phosphate dodecahydrate ($Na_2HPO_4{\cdot}12H_2O$) and Sodium dihydrogen phosphate dihydrate ($NaH_2PO_4{\cdot}2H_2O$) were purchased from Sigma (St. Louis, MO, USA). Other reagents were all of analytical grade.

The sodium phosphate buffer containing 20 mM disodium hydrogen phosphate dodecahydrate was adjusted to pH 7.4 with 20 mM sodium dihydrogen phosphate dihydrate. Individual stock standard was prepared with ethanol for 3 mM ligustroflavone. A 100 μM BSA stock solution was daily prepared by dissolving an appropriate amount of BSA with 20 mM sodium phosphate buffer. For ACE, sample solution was obtained daily by dilution with the phosphate buffer from the corresponding stock solution to a final concentration of 150 μM before analysis. In sample solution, 3% acetone was used as an EOF marker. Working BSA solutions (0–14 μM) were obtained by diluting BSA stock solutions with sodium phosphate buffer containing 0.1 M glycine (Gly). For the fluorescence measurement, the concentration of BSA was fixed at 2 μM in 20 mM phosphate solution containing 0.1 M NaCl (pH = 7.4) and the ratio of ligustroflavonet to BSA were 0, 1, 2, 3, 4, 5, 6, 7, 8, 9 and 10, respectively. During the UV spectrum analysis, the ligustroflavonet concentration was 0–30 μM while the BSA concentration was fixed at 10 μM. All solutions were filtered through 0.22 μM filters and stored at 4 °C.

2.3. Procedures

A new capillary was rinsed for 5 min with 1M NaOH, and then, conditioned with water for 10 min and with the phosphate buffer for 15 min. In order to obtain great peak shape and reproducibility, the capillary was rinsed for 3 min with 0.1 M NaOH solution, 3 min with water, and 3 min with buffer, all at 20 psi between two injections.

The sample solution was introduced into the capillary by hydrodynamic injection (0.5 psi for 5 s). The detection wavelength was 336 nm. The applied voltage was set to 15 kV. In the ACE analysis, the electrophoresis was carried out with 20 mM phosphate buffer (pH 7.4, 0.1 M

Gly) containing different concentrations of BSA (0–14 μM). In order to eliminate the effect of protein adsorption on the capillary inner wall, Gly was added to the buffer solution. Gly, an amphotericion, can suppress protein adsorption by competing with BSA to adsorb onto the capillary inner wall. Besides, the BSA concentration was low in this work which were controlled in the range of 0 to 14 μM. In fluorescence experiments, 2 μM BSA solution was titrated with different ligustroflavone concentrations (0, 2, 4, 6, 8, 10, 12, 14, 16, 18, 20 μM). Fluorescence spectra were recorded at 298 K in the range of 295–600 nm upon excitation at 280 nm. The spectral bandwidths of both the excitation slit and the emission slit were set to 10.0 nm. UV-Vis absorption spectra of the BSA and the BSA-ligustroflavone mixtures were acquired by keeping BSA concentration constant at 10 μM and varying ligustroflavone concentration (0–30 μM) in the range of 200 to 500 nm at 298 K.

3. RESULTS AND DISCUSSION

3.1. Theory of the estimation of binding constants by ACE method

For drug/protein interaction studies, either the drug or the protein can be added into the ACE running buffer. In this work, considering the cost of drugs, protein was used as an additive in the running buffer and the drug concentration was fixed as constant. The binding reaction and binding constant (*Ka*) of between the drug (*D*) and serum albumin (*P*) can be expressed by the following equation (Eq.) assumed that a 1:1 complex (*DP*) is formed [28, 29].

$$D + P = DP$$

$$Ka = [DP]/[D][P], \qquad (1)$$

where [*D*], [*P*], [*DP*] are the concentrations of the drug, serum albumin and drug-protein complex. The following Scatchard equation (2) was applied to calculate *Ka* [30].

$$1/\Delta\mu_D^P = \left[1/(Ka \times \Delta\mu_{\max}) \times 1/C(P)\right] + 1/\Delta\mu_{\max},$$

$$\Delta\mu_D^P = \mu_D^P - \mu_D, \qquad (2)$$

where μ_D^P and μ_D is the electrophoretic mobility of drugs in the presence and absence of protein. $\Delta\mu_{\max} = \mu_{DP} - \mu_D$, where μ_{DP} is the mobility of the complex. Linear graphs were obtained by plotting $1/\Delta\mu_D^P$ against $1/c(P)$. Thus, the binding constant was the intercept/slope ratio of the linear graph. But there were limitations to the method of analysis as protein was added in the buffer. The EOF and the viscosity of the buffer could change with the various concentration of the protein and cause a large discrepancy of *Ka* [31]. To eliminate the influences, the mobility ratio (*M*) was introduced [32]. *M* has been proven to be not related to the working voltage and buffer viscosity, so it was found to give more precise estimates of the *Ka*. The calculation of *M* is as following [33]:

$$M = \left(\mu_{eo} + \mu_D^P\right)\Big/\mu_{\text{eo}} = t_{eo}/t_D^P + 1, \qquad (3)$$

where t_{eo} is the migration time of the EOF and t_D^P is the migration time of the analyte, so that the Scatchard equation is changed to Eq. (4) [3].

$$1/\Delta M_D^P = \left[1/(Ka \times \Delta M_{\max}) \times 1/c(P)\right] + 1/\Delta M_{\max},$$

$$\Delta M_D^P = M_D^P - M_D, \quad \Delta M_{\max} = M_{DP} - M_D, \qquad (4)$$

where M_D^P and M_D are the drug mobility ratio in the presence and absence of protein. And the M_{DP} is the mobility ratio of the complex. In this study, Scatchard analysis was performed using Eq. 4 and linear fit was done to obtain the estimated *Ka* value.

3.2. Measurement of the drug/BSA binding constant by ACE

The migration time (t_D^P) of ligustroflavone were measured in the present of different BSA concentrations of the buffers in Table 1. A set of electropherograms of the ligustroflavone versus BSA concentration change at 298 K were shown in Fig. 2. From the electropherograms and the time data, it could be found that the peaks of ligustroflavone and acetone shifted to the right with the increase of BAS concentrations. The complexation between ligustroflavone and BSA resulted in an increase of the complex *m/z* ratio was detected later than the uncomplexed form. And peak shape of ligustroflavone gradually became asymmetric as the BSA concentrations increased. Table 2 lists the

Table 1. Migration time of ligustroflavone obtained by ACE method and their transformation

$c(P)$, μM	t_R, min	t_D^P, min	ΔM_D^P	$1/\Delta M_D^P$	$1/c(P)$, μM^{-1}
0	5.729	5.938			
2	7.283	7.592	−0.0114	−87.7192	0.5000
4	7.633	8.037	−0.0151	−66.2252	0.2500
6	9.079	9.683	−0.0272	−36.7647	0.1667
10	9.979	10.738	−0.0355	−28.1690	0.1000
12	11.679	12.704	−0.0455	−21.9780	0.0833
14	12.154	13.308	−0.0515	−19.4175	0.0714

Table 2. The Ka and Scatchard equation of ligustroflavone–protein at different temperatures

	T, K	Scatchard equation	K_a, M^{-1}	R^2
ligustroflavone	298	$y = -162.88x - 11.5790$	7.1089×10^4	0.9340
	303	$y = -181.9x - 7.2035$	3.9601×10^4	0.9961
	308	$y = -239.85x - 2.2952$	0.9569×10^4	0.9777

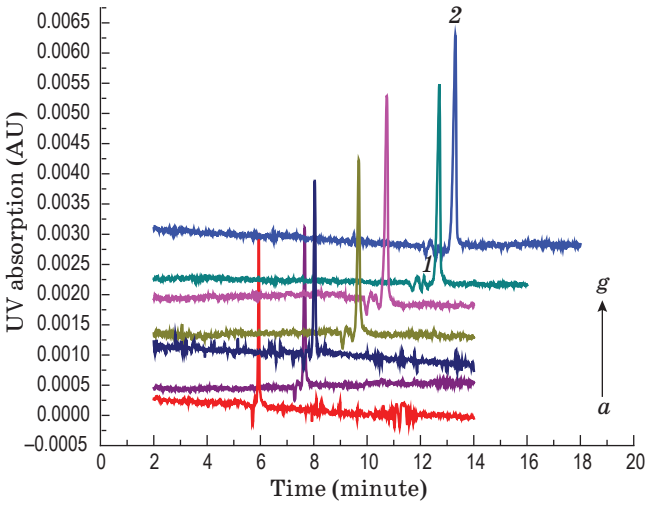

Fig. 2. Electropherograms of ligustroflavone in the presence of different BSA concentrations in 20 mM phosphate buffer (pH = 7.4, 0.1 M Gly) at 298 K. a-g represent BSA concentration of 0, 2, 4, 6, 10, 12 and 14 μM. The concentration of ligustroflavone was150 μM. Peak *1* — acetone, *2* — ligustroflavone.

Scatchard equation and the calculated *Ka* estimated by the intercept/slope ratio of ligustroflavone with BSA at different temperature. The binding affinity gradually decreased as the temperature increased while the *Ka* was decreased from 7.1089×10^4 to 9.569×10^3. The data shows a linear relationship with coefficients from 0.9340 to 0.9961 for ligustroflavone-protein.

3.3. Affinity measurements using fluorescence spectroscopy

To obtain more information about the structural perturbation of BSA, fluorescence quenching experiment was performed. The interaction of ligustroflavone with BSA was evaluated by monitoring the intrinsic fluorescence intensity changes of BSA upon addition of ligustroflavone. The mechanisms of quenching are usually classified as either dynamic quenching or static quenching. Dynamic quenching refers to a process that the fluorophore and the quencher come into contact during the transient existence of the excited state. Static quenching refers to fluorophore-quencher complex formation. To clarify the fluorescence quenching mechanism of BSA with ligustroflavone, it was first assumed that the binding process is a dynamic way. Regression curves were plotted according to the Stern–Volmer Eq. (5) [34, 35].

$$F_0/F = 1 + K_Q \times \tau_0 \times [Q] = 1 + K_{SV} \times [Q], \quad (5)$$

where F_0 and F are the fluorescence intensities of BSA before and after the addition of the ligustroflavone, respectively. And K_Q is the quenching rate constant of the ligustroflavone, K_{SV} is the Stern–Volmer dynamic quenching constant, τ_0 is the average lifetime of the biomolecule without quencher ($\tau_0 = 10^{-8}$ s [36, 37]), and $[Q]$ is the concentration of quencher. K_{SV} and K_Q

Table 3. Stern–Volmer quenching constants and binding parameters for the interaction of BSA with ligustroflavone at 298 K

	Stern–Volmer quenching constants			Binding parameters		
T	K_{SV}, M^{-1}	K_Q, $M^{-1}\cdot s^{-1}$	R^2	Kb, M^{-1}	n	R^2
298 K	4.38×10^4	4.38×10^{12}	0.9598	8.0057×10^4	1.0688	0.9654

were calculated at 298 K according to Eq. 5. The results showed that the K_Q (4.38×10^{12}) is much greater than the maximum scattering collision quenching constant (2.0×10^{10} $M^{-1}\cdot s^{-1}$ [38, 39]), which indicated that the possible quenching mechanism is not the result of dynamic quenching, but static quenching by complex formation. The static quenching equation can be described by the binding constant Eq. 6 [1, 40, 41]

$$\log_{10}\left[(F_0-F)/F\right]=\log_{10}(Kb)+n\log_{10}[Q], \quad (6)$$

where Kb is the binding constant of ligustroflavone with BSA which can be determined by the slope of double logarithm regression curve of $\log_{10}[(F_0-F)/F]$ versus $\log_{10}[Q]$ based on the Eq. (6) and n is the number of binding sites per BSA. The mean of F_0, F and Q were the same as those in equation 5. The fluorescence spectra of BSA with different concentrations of ligustroflavone are shown in Fig. 3. As the concentration of ligustroflavone increased gradually, the fluorescence intensity of BSA decreased, indicating that ligustroflavone has an obvious quenching effect on BSA. The experimental results of static quenching are listed in Table 3. The binding constant and the binding sites number between static quenching and ACE are generally the same. The slight difference may be caused by the difference of sensitivity and error of the methods.

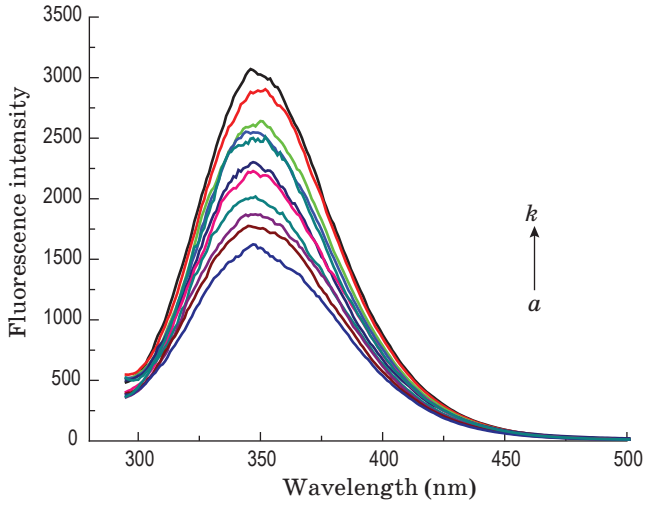

Fig. 3. Fluorescence spectra of the BSA-ligustroflavone system. The concentration of BSA was 2.0 μM and ligustroflavone concentration increased from 0 to 20 μM at 298 K, a-k: 0, 2, 4, 6, 8, 10, 12, 14, 16, 18 and 20 μM, respectively.

3.4. UV-Vis absorption spectroscopy

To clarify the probable fluorescence quenching mechanism of BSA by ligustroflavone, the UV-Vis absorption spectra of BSA and the mixture of BSA-ligustroflavone were recorded at 298 K (Fig. 4). It is obvious that the intensity of UV-Vis absorption of BSA enhances with the increase of ligustroflavone concentration. Its showed that the possible quenching mechanism between ligustroflavone and BSA was static quenching by forming the complex.

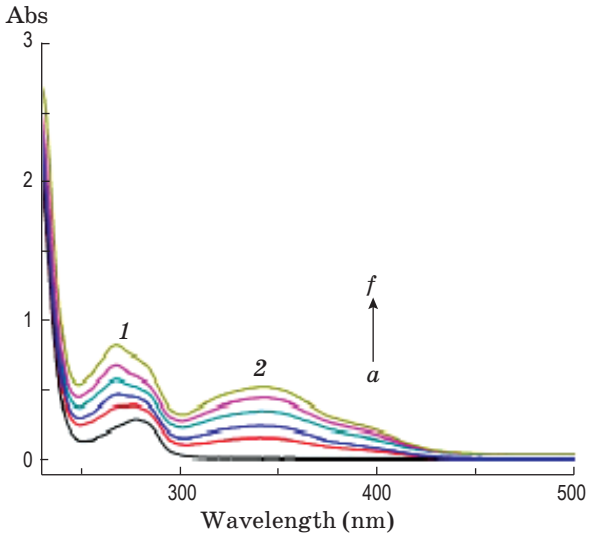

Fig. 4. UV-Vis absorption spectra of BSA in the presence of ligustroflavone. The concentration of BSA was 10 μM and ligustroflavone concentration increased from 0 to 30 μM at 298 K. a-f: 0, 10, 15, 20, 25, and 30 μM, respectively. Peak *1* — BSA-ligustroflavone, *2* — ligustroflavone.

Table 4. Thermodynamic parameters of the ligustroflavone–protein binding process at different temperatures

	T, K	ΔH, KJ·M^{-1}	ΔS, KJ·M^{-1}	ΔG, KJ·M^{-1}
ligustroflavone	298	−152.6700	−0.4194	−27.6786
	303		−0.4158	−26.6690
	308		−0.4195	−23.4723

3.5. Analysis of interaction forces by ACE method

Generally, the interaction forces between small molecules and protein mainly involve several forces, including hydrogen bonds, van der Waals forces, electrostatic interactions, and hydrophobic interactions [19]. In this process, the thermodynamic parameters of enthalpy change (ΔH), entropy change (ΔS), and free energy change (ΔG) of the reaction, are important for estimation and confirming binding mode of drug-protein. Considering that ΔH can be regarded as constant, thermodynamic parameters of the binding procedure were calculated using the following equations [42, 10]:

$$\ln Ka = \left(-\Delta H/RT\right) + \Delta S/R, \quad (7)$$

$$\Delta G = -RT \ln K, \quad (8)$$

$$\Delta S = \left(\Delta H - \Delta G\right)/T, \quad (9)$$

where Ka is the binding constant at the corresponding temperature and R is the gas constant. To examine the binding model of ligustroflavone with BSA, the thermodynamic parameters of the interaction process were investigated at 298, 303 and 308 K by ACE method. The obtained thermodynamic parameters were listed in Table 4. As we can see, the negative values of ΔG suggested that the interaction process was spontaneous for ligustroflavone with BSA. The negative ΔS and ΔH is frequently taken as evidence for Van der Waals forces [36]. The negative ΔH value was also observed whenever there were hydrogen bonds and exothermic process. The positive ΔS value is frequently taken as evidence for hydrophobic interactions. And a positive value of ΔS along with a negative ΔH value (near zero) was characteristic of electrostatic interactions in aqueous solution [18].

4. CONCLUSION

The interaction between ligustroflavone and BSA was investigated by ACE, fluorescence spectroscopy and UV-Vis absorption spectroscopy. The binding constant by fluorescence quenching is 8.0057×10^4 for ligustroflavone with BSA. The result is basically consistent with that found by ACE, in which the binding constants are 7.1089×10^4. It indicates that ligustroflavone has strong binding ability to BSA. The fluorescence quenching mechanism for BSA through ligustroflavone binding is likely a static quenching process which was evident from the data of biomolecule quenching rate constant K_Q and the UV-Vis absorption spectra. The number of binding sites n was approximately one which is in accordance with experimental hypothesis. Thermodynamic parameters obtained by ACE method showed that both van der Waals interaction and hydrogen bonds played vital roles in the binding process of ligustroflavone to BSA. In fact, protein adsorption onto the capillary inner wall is a big hindrance for the use of ACE to assess biological binding. However, nonspecific adsorption of protein does not affect fluorescence analysis, so the results obtained from fluorescence spectroscopy can be used to validate the value from ACE. The agreement between ACE and fluorescence on high affinity binding sites suggests that these two techniques are comparable for binding studies. Meanwhile, UV-Vis absorption measurement is a simple but effective method in detecting complex formation, which can further demonstrate the reliability of fluorescence spectral data. This study can help us to understand pharmacokinetic and pharmacodynamic properties of ligustroflavone.

Author would like to thank the financial support of Natural Science Foundation of Shandong Province (Grant No. ZR2018LB021).

REFERENCES

1. *He T.X., Liang Q.L., Luo T.T., Wang Y.M., Luo G.A.* Study on interactions of phenolic acid-like drug candidates with bovine serum albumin by capillary electrophoresis and fluorescence spectroscopy // J. Solution Chem. 2010. V. 39(11). P. 1653–1664.
2. *Xiang Y.H., Duan L.L., Ma Q., Lv Z.Z., Zhu R.H, Zhang Z.Y.* Fluorescence spectroscopy and molecular simulation on the interaction of caffeic acid with human serum albumin // Lumin. 2016. V. 31 (8). P. 1496–1502.
3. *Xu Y.J., Hong T.T., Chen X.P., Ji Y.B.* Affinity capillary electrophoresis and fluorescence spectroscopy for studying enantioselective interactions between omeprazole enantiomer and human serum albumin // Electrophoresis. 2017. V. 38 (9–10). P. 1366–1373.
4. *Zhang Y.L., Sha Y.J., Qian K., Chen X., Chen Q.* Comparison of three methods for analyzing loureirin B and human serum albumin interaction using capillary electrophoresis // Electrophoresis. 2017. V. 38(7). P. 1038–1043.
5. *Minic S., Stanic-Vucinic D., Radomirović M., Radibratovic M., Nikolic M., Cirkovic Velickovic T.* Characterization and effects of binding of food-derived bioactive phycocyanobilin to bovine serum albumin // Food Chem. 2018. V. 239. P. 1090–1099.
6. *Wani T.A., Bakheit A.H., Abounassif M.A., Zargar S.* Study of interactions of an anticancer drug neratinib with bovine serum albumin: spectroscopic and molecular docking approach // Front. Chem. 2018. V. 6(47). P. 1–9.
7. *Shi J.H., Pan D.Q., Wang X.X., Liu T.T., Jiang M., Wang Q.* Characterizing the binding interaction between antimalarial arte-mether (AMT) and bovine serum albumin (BSA): spectroscopic and molecular docking methods // J. Photoch. Photobio. B. 2016. V. 162. P. 14–23.
8. *Roy S., Nandi R.K., Ganai S., Majumdarb K.C., Dasa T.K.* Binding interaction of phosphorus heterocycles with bovine serum albumin: A biochemical study // J. Pharm. Anal. 2017. V. 7(1). P. 19–26.
9. *Dominguez M., Cortes-Figueroa J.E., Melendez E.* Biological interaction of Molybdenocene dichloride with bovine serum albumin using fluorescence spectroscopy // J. Chem. Educ. 2018. V. 95(1). P. 152–157.
10. *He T.X., Liang Q.L., Wang Y.M., Luo G.A.* Characterization of the interactions between natural flavonoid compounds and bovine serum albumin by capillary electrophoresis and fluorescence method // J. Liq. Chromatogr&R. 2010. T. 33(4). P. 548–562.
11. *Ma S.G., Yuan S.P., Hou Q.* Study on flavonoid glycosides and their anti-inflammatory activities in the Folium Turpinia // J. Tradit. Chin. Med. 2013. V. 38(11). P. 1747–1750.
12. *Zhang L., Li J., Yu S.C., Jin Y., Lu X.W., Li Y.* Therapeutic effects and mechanisms of total flavonoids of Turpinia Arguta Seen on adjuvant arthritis in rats // J. Ethnopharmacol. 2008. V. 116(1). P. 167–172.
13. *Zhang L., Li J., Yu S.C., Jin Y., Lu X.W., Peng L.* Effect of total flavonoids from Shan Xiang Yuan on immune function of adjuvant arthritis in rats // Chin. Pharmacol. Bull. 2007. V. 23(1). P. 106–110.
14. Chinese Pharmacopoeia Commission. Pharmacopoeia of the People's Republic of China. Part 1. Beijing: China Medical Science Press, 2010. P. 28.
15. *Asensi-Bernardi L., Martín-Biosca Y., Escuder Gilabert L., Sagrado S., Medina-Hernández M.J.* Evaluation of the enantioselective binding of imazalil to human serum albumin by capillary electrophoresis // Biomed. Chromatogr. 2015. V. 29(11). P. 1637–1642.
16. *Zhang J., Chen L.N., Zeng B.R., Kang Q.L., Dai L.Z.* Study on the binding of chloroamphenicol with bovine serum albumin by fluorescence and UV-vis spectroscopy // Spectrochim. Acta A. 2013. V. 105(1). P. 74–79.
17. *Yue Y.Y., Chen X.G., Qin J., Yao X.J.* Characterization of the mangiferin-human serum albumin complex by spectroscopic and molecular modeling approaches // J. Pharm. Biomed. Anal. 2009. V. 49(3). P. 753–759.
18. *Tayyab S., Mirza Izzudin M., Kabir M.Z., Feroz S.R., Tee W.V., Mohamad S.B., Alias Z.* Binding of an anticancer drug, axitinib to human serum albumin: Fluorescence quenching and molecular docking study // J. Photoch. Photobio. B. 2016. V. 162. P. 386–394.
19. *Li Y., Chen C., Zhang C.P., Duan J.Y., Yao H.K., Wei Q.L.* Probing the binding interaction of AKR with human serum albumin by multiple fluorescence spectroscopy and molecular modeling // J. Biomol. Struct. Dyn. 2017. V. 35(6). P. 1189–1199.
20. *Fotouhi L., Banafsheh S., Heravi M.* Electrochemistry of the interaction of furazolidone and bovine serum albumin // Bioelectrochemistry. 2009. V. 77(1). P. 26–30.
21. *Deeb S.E., Wätzig H., El-Hady D.A., Albishri H.M., De Griend C.S.V., Scriba G.K.E.* Recent advances in capillary electrophoretic migration techniques for pharmaceutical analysis // Electrophoresis. 2014. V. 35(1). P. 170–189.

22. *Wätzig H., Oltmann-Norden I., Steinicke F., Alhazmi H.A., Nachbar M., El-Hady D.A., Albishri H.M., Baumann K., Exner T., Böckler F.M., Deeb S.E.* Data quality in drug discovery: the role of analytical performance in ligand binding assays // J. Comput. Aid. Mol. Des. 2015. V. 29(9). P. 847–865.

23. *Mais O., Matthias S., Hermann W.* Affinity capillary electrophoresis for studying interactions in life sciences // Methods. 2018. V. 146. P. 76–92.

24. *Zhang Y.T., Xu M.T., Du M., Zhou F.M.* Comparative studies of the interaction between ferulic acid and bovine serum albumin by ACE and surface plasmon resonance // Electrophoresis. 2010. V. 28(11). P. 1839–1845.

25. *Mozafari M., El Deeb S., Krull F., Wildgruber R., Weber G., Reiter C.G., Wätzig H.* Interaction of albumins and heparinoids investigated by affinity capillary electrophoresis and free flow electrophoresis // Electrophoresis. 2018. V. 39(4). P. 569–580.

26. *Deeb S.E., Wätzig H., El-Hady D.A., De Griend C.S.V., Scriba G.K.E.* Recent advances in capillary electrophoretic migration techniques for pharmaceutical analysis (2013–2015) // Electrophoresis. 2016. V. 37. P. 1591–1608.

27. *Zhu M.Q., Wang L.J., Wang Y., Zhou J., Ding J., Li W., Xin Y., Fan S.S., Wang Z., Wang Y.* Biointeractions of herbicide atrazine with human serum albumin: UV-Vis, fluorescence and circular dichroism approaches // Int. J. Environ. Res. Public. Health. 2018. V. 15(1). P. 116–131.

28. *Michalcová L., Zdenek G.* Study on the interactions of sulfonylurea antidiabetic drugs with normal and glycated human serum albumin by capillary electrophoresis-frontal analysis // J. Sep. Sci. 2016. V. 39(18). P. 3631–3637.

29. *Qian C., Wang S., Fu H.Q., Turner R.F.B., Li H.H., Chen D.D.Y.* Pressure-assisted capillary electrophoresis frontal analysis for faster binding constant determination // Electrophoresis. 2018. V. 39(14). P. 1786–1793.

30. *Zhang B., Li Y.X., Gao H.N., Bian J., Bao J.J.* Rapid determination of protein binding constant by a pressure-mediated affinity capillary electrophoresis method // Electrophoresis. 2011. V. 32(24). P. 3589–3596.

31. *Liu X.P., Du Y.X.* Study on the binding of chiral drug duloxetine hydrochloride to human serum albumin // Eur. J. Med. Chem. 2010. V. 45(9). P. 4043–4049.

32. *Bose S., Yang J., Hage D.S.* Guidelines in selecting ligand concentrations for the determination of binding constants by affinity capillary electrophoresis // J. Chromatogr. B. 1997. V. 697(1–2). P. 77–88.

33. *Liu C.Y., Wei Y.M., Miao Y.Q., Zhang Y.Y.* Interactions between isoprenaline hydrochloride and bovine serum albumin (BSA) in capillary zone electrophoresis and affinity capillary electrophoresis // Pharmazie. 2012. V. 67(10). P. 839–843.

34. *Wang Y., Zhu M.Q., Liu F., Wu X.W., Pan D.D., Liu J., Fan S.S., Wang Z., Tang J., Na R., Li Q.X., Hua R., Liu S.Z.* Comparative studies of interactions between fluorodihydroquinazolin derivatives and human serum albumin with fluorescence spectroscopy // Molecules. 2016. V. 21(10). P. 1373–1386.

35. *Makarska-Bialokoz M.* Interactions of hemin with bovine serum albumin and human hemoglobin: A fluorescence quenching study // Spectrochim. Acta A. 2017. V. 193. P. 23–32.

36. *Li G.X., Liu B.S., Zhang Q.J., Han R.J.* Investigation on the effect of fluorescence quenching of bovine serum albumin by cefoxitin sodium using fluorescence spectroscopy and synchronous fluorescence spectroscopy // Lumin. 2015. V. 31(5). P. 1054–1062.

37. *Sharma A.S., Anandakumar S., Ilanchelian M.* A combined spectroscopic and molecular docking study on site selective binding interaction of to luidine blue O with human and bovine serum albumins // J. Lumin. 2014. V. 151(151). P. 206–218.

38. *Asadi M., Asadi Z., Zarei L., Sadi S.B., Amirghofran Z.* Affinity to bovine serum albumin and anticancer activity of some new water-soluble metal Schiff base complexes // Spectrochim. Acta A. 2014. V. 133. P. 697–706.

39. *Cheng X.X., Fan X.Y., Jiang F.L., Liu Y., Lei K.L.* Resonance energy transfer, pH-induced folded states and the molecular interaction of human serum albumin and icariin // Lumin. 2015. V. 30(7). P. 1026–1033.

40. *Zhou N., Liang Y.Z., Wang B., Wang P., Chen X., Zeng M.M.* Interaction of glycyrrhetinic acid, furosemide and hydrochlorothiazide with bovine serum albumin // Biomed. Chromatogr. 2008. V. 22. P. 223–231.

41. *Tian Z.Y., Zang F.L., Luo W., Zhao Z.H., Wang Y.Q., Xu X.J., Wang C.J.* Spectroscopic study on the interaction between mononaphthalimide spermidine (MINS) and bovine serum albumin (BSA) // J. Photoch. Photobio. B. 2015. V. 142. P. 103–109.

42. *Yang J., Jing Z.H., Jie J.J., Guo P.* Fluorescence spectroscopy study on the interaction between Gossypol and bovine serum albumin // J. Mol. Struct. 2009. V. 920(1–3). P. 227–230.